

L. Vočadlo · K. S. Knight · G. D. Price · I. G. Wood

## Thermal expansion and crystal structure of FeSi between 4 and 1173 K determined by time-of-flight neutron powder diffraction

Received: 22 January 2001 / Accepted: 2 July 2001

**Abstract** The thermal expansion and crystal structure of FeSi has been determined by neutron powder diffraction between 4 and 1173 K. No evidence was seen of any structural or magnetic transitions at low temperatures. The average volumetric thermal expansion coefficient above room temperature was found to be  $4.85(5) \times 10^{-5} \text{ K}^{-1}$ . The cell volume was fitted over the complete temperature range using Grüneisen approximations to the zero pressure equation of state, with the internal energy calculated via a Debye model; a Grüneisen second-order approximation gave the following parameters:  $\theta_{\text{D}} = 445(11) \text{ K}$ ,  $V_0 = 89.596(8) \text{ \AA}^3$ ,  $K'_0 = 4.4(4)$  and  $\gamma' = 2.33(3)$ , where  $\theta_{\text{D}}$  is the Debye temperature,  $V_0$  is  $V$  at  $T = 0 \text{ K}$ ,  $K'_0$  is the first derivative with respect to pressure of the incompressibility and  $\gamma'$  is a Grüneisen parameter. The thermodynamic Grüneisen parameter,  $\gamma_{\text{th}}$ , has been calculated from experimental data in the range 4–400 K. The crystal structure was found to be almost invariant with temperature. The thermal vibrations of the Fe atoms are almost isotropic at all temperatures; those of the Si atoms become more anisotropic as the temperature increases.

**Keywords** FeSi · Thermal expansion · Crystal structure · Neutron diffraction

### Introduction

Iron monosilicide,  $\epsilon$ -FeSi, is a material of considerable interest to crystallographers, physicists and Earth and planetary scientists. It crystallises with an unusual cubic structure (space group  $P2_13$ ,  $Z = 4$ ) in which each species lies in sevenfold coordination (Pauling and Soldate 1948). Both Fe and Si atoms occupy  $4a(x, x, x)$  sites on threefold axes. If  $x = \pm 0.15451$  then the sevenfold coordination is ideal with all coordinating atoms equidistant. The details of the structure have been discussed by Wood et al. (1996), Vočadlo et al. (1999, 2000) and Mattheiss and Hamann (1993). The electrical and magnetic properties have a number of interesting and unusual features including the possibility of electrical and magnetic transformations at very low temperatures (Paschen et al. 1997; Sluchanko et al. 1998). The chief interest to Earth and planetary scientists arises from the possibility that silicon might be an alloying element in the Earth's core; the material has also been suggested very recently as a circumstellar dust component (Ferrarotti et al. 2000). A number of both experimental and theoretical studies of the incompressibility of the material have been made (reviewed in Vočadlo et al. 1999, 2000). In general, computer simulations have predicted an incompressibility much higher than the experimentally determined values. The reason for this discrepancy is not yet clear, although there is some possibility that it could be due to some form of magnetic ordering or other phase transition at low temperatures (all of the computer studies of the material have been static, athermal simulations, i.e. at 0 K), a hypothesis suggested by the results of Sluchanko et al. (1998) and Paschen et al. (1997). Although the magnetisation of FeSi has been the subject of a number of neutron scattering studies (Shirane et al. 1987; Tajima et al. 1988), these have been primarily concerned with investigations of the unusual paramagnetism shown by the material at and above room temperature. No structural studies have been carried out at low temperatures other than a

L. Vočadlo (✉) · G. D. Price · I. G. Wood  
Department of Geological Sciences,  
University College London,  
Gower Street, London, WC1E 6BT, UK  
e-mail: l.vocadlo@ucl.ac.uk  
Fax: +44-20-7387-1612

K. S. Knight  
ISIS Facility, Rutherford Appleton Laboratory, Chilton,  
Didcot, Oxon OX11 0QX, UK and

Department of Mineralogy,  
The Natural History Museum,  
Cromwell Road, London, SW7 5BD, UK

neutron powder diffraction experiment at liquid nitrogen temperature by Watanabe et al. (1963). No measurements of the thermal expansion of the material have been reported. Time-of-flight powder neutron diffraction provides an ideal method to determine the structure and thermal expansion as a function of temperature. For a simple inorganic structure with a small unit cell, such as FeSi, accurate positional and thermal parameters may be obtained by Rietveld refinement. The time-of-flight technique has the considerable advantage that accurate lattice constants may be obtained from high-intensity, large  $d$ -spacing reflections, enabling short data collection times which, in turn, allow a detailed investigation of the structure over a very wide range of temperatures.

In this paper, therefore, we present the results of a study of the crystal structure of FeSi between 4.2 and 1173 K, together with thermoelastic properties of the material, obtained using Grüneisen approximations to the zero pressure equation of state.

## Experimental methods

The material used in the present study (obtained from the Technical Glass Company, Cambridge) had been prepared by reaction of a stoichiometric mixture of iron (99.998% purity) and silicon (99.9999% purity) under argon gas. The powder sample was prepared by breaking the boule supplied in a percussion mortar, sieving the resulting material through a 30-mesh (0.5-mm) sieve and grinding this fraction for 5 min with distilled water in a McCrone micronising mill using agate grinding elements. An X-ray powder diffraction pattern of this material, collected using a Philips PW1050 vertical goniometer with Fe-filtered  $\text{CoK}\alpha$  radiation, showed little evidence of any impurity phases, except for a very small reflection (less than 0.5% in height relative to the strongest peak in FeSi pattern) with a  $d$ -spacing of  $\sim 1.15$  Å, which would correspond to the strongest peak from both  $\text{Fe}_2\text{Si}$  and  $\text{Fe}_3\text{Si}$ .

The neutron diffraction data were collected using the POLARIS powder diffractometer at the ISIS neutron spallation source of the Rutherford-Appleton Laboratory. POLARIS is a high-flux, medium-resolution instrument with low-angle,  $90^\circ$  and high-angle detector banks (Hull et al. 1992). The prepared sample was divided into two subsamples for use in the high- and low-temperature experiments. For the high-temperature study, the sample was placed under vacuum (nominally 10 mPa) in an 11-mm diameter vanadium can, which in turn was placed in a standard ISIS furnace with vanadium windings. Data were collected on heating in  $\sim 25$  K intervals between 373 and 1173 K; for most datasets a counting time of  $\sim 15$  min was used after an initial 5-min temperature equilibration period. The data at 373, 773, 973 and 1173 K were counted for a longer period ( $\sim 45$  min) to allow more precise refinements of the structures. For the low-temperature study a similar can was used in an ILL-Orange cryostat. In this case, data were collected at 4.2 K for  $\sim 1.5$  h, and then from nominally 10–100 K in 5-K steps and from 100–300 K in 10-K steps, each for a duration of  $\sim 15$  min; temperature equilibration periods of 5 and 10 min, respectively, were used for the two stages of the experiment. Figure 1a shows representative datasets covering the full range of temperature. For both the cryostat and furnace data, the actual temperatures corresponding to each point were obtained by averaging the readings in the temperature log file.

The neutron patterns obtained at temperatures above 973 K showed some weak additional peaks (see Fig. 1a) which persisted when the sample was cooled. Subsequent analysis by X-ray diffraction of the recovered sample at room temperature indicated that these corresponded to the strongest reflections from  $\text{Fe}_2\text{SiO}_4$ ,

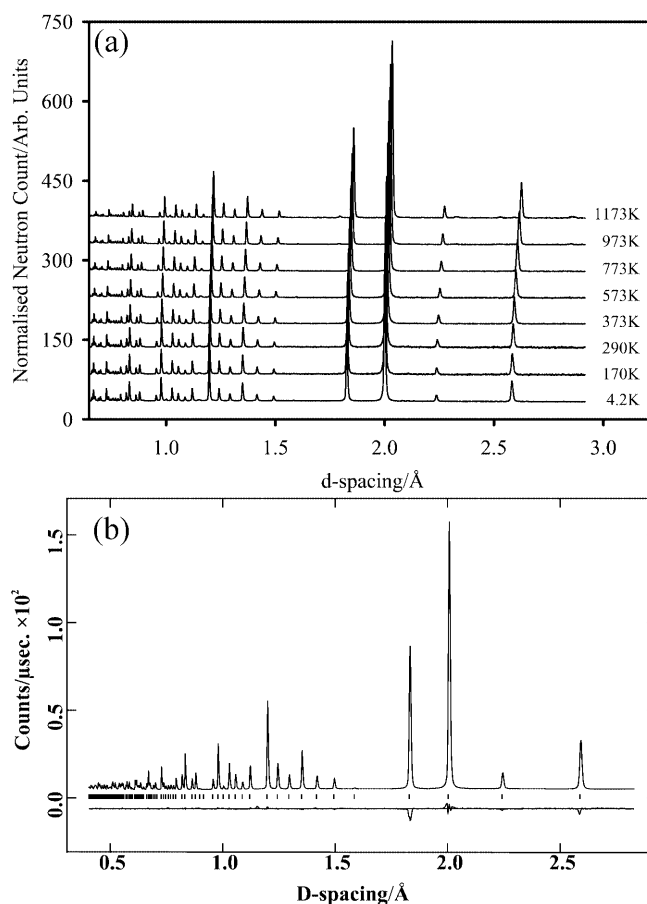


**Fig. 1** **a** Neutron powder diffraction patterns from FeSi at temperatures of nominally 4.2, 170, 290, 373, 573, 773, 973 and 1173 K. The weak extra reflections on the patterns at 973 and 1173 K (e.g. at 1.80, 2.33, 2.53 and 2.87 Å) are due to  $\text{Fe}_2\text{SiO}_4$  (see text). **b** Observed and calculated diffraction patterns for FeSi at room temperature (291 K). At the resolution of this figure, the two patterns are indistinguishable to the naked eye, but the lower trace shows the difference between them (Observed-Calculated). The vertical bars indicate the positions of the expected Bragg reflections

with an intensity ratio between the strongest  $\text{Fe}_2\text{SiO}_4$  and FeSi peaks of  $\sim 0.7\%$ . Oxidation of the sample was, perhaps, unexpected, given the high vacuum under which it was held when in the furnace. In view of the low intensity and lack of overlap of these peaks with those of FeSi, the presence of this impurity phase was ignored in the analysis of the neutron data, none of the derived parameters showing any systematic change in behaviour above 973 K. The structure refinements from the neutron diffraction patterns were carried out using the program GSAS (Larson and Von Dreele 1994) to fit the data from the backscattering detectors, with flight times between 2.5 and 17.5 ms, corresponding to a  $d$ -spacing range of 0.40–2.83 Å; a total of 21 parameters were included in the refinements (cell parameter, scale factor, extinction coefficient, two peak profile parameters, six structural parameters and ten background parameters). Anisotropic thermal parameters were used, as it was felt that the  $d$ -spacing range available was such that meaningful values could be obtained. The weighted profile  $R$  factors for the refinements were typically  $< 3\%$ . The observed and calculated diffraction patterns for the refinement at room temperature are shown in Fig. 1b.

The cell volumes from the furnace and cryostat experiments were found to be not identical at room temperature. The two

datasets were brought into coincidence by applying a scaling factor (0.99973) to the high-temperature data; this factor was obtained from the ratio of the cell parameters at room temperature. The offset arises from a slight difference in the position of the sample in the two experiments; the magnitude of the scaling factor is equivalent to a difference in sample position of 3.5 mm in the  $\sim 13$  m flight path of POLARIS.

## Results and discussion

### Possible phase transitions at low temperatures

It is clear from Fig. 1a that the cubic  $\epsilon$ -FeSi structure persists over the full temperature range of the experiments. We were unable to detect any evidence in the diffraction pattern of the spin density wave transition suggested to occur at  $\sim 7$  K by Sluchanko et al. (1998), and the temperature range used in the present experiments was insufficient to be able to detect any consequences of the metal-insulator transition reported at very low temperatures ( $< 4$  K) by Paschen et al. (1997). Careful comparison of the diffraction patterns from the low-angle detectors ( $d$ -spacing range 0.5–8.25 Å) at 4.2 and 100 K showed no evidence of any extra peaks or long-wavelength periodic structure in the background, although there remains the possibility that the magnetic anomaly could be observed at smaller scattering vector (i.e. longer wavelength). There is little evidence of magnetostriction in the present experiment although there is possibly a slight alteration in the slope of the  $V$ – $T$  curve below 15 K; however, to determine whether this effect truly exists would require a more detailed examination of the behaviour of the lattice parameter below 10 K using a higher resolution machine such as HRPD at ISIS.

### Thermal expansion and thermoelastic properties

Figure 2 shows the variation of volume with temperature over the entire temperature range covered in the two experiments. The standard deviation of the cell parameters obtained from the results of the Rietveld refinements was 0.00002 Å for all datasets; this value leads to a constant error in the volumes of 0.001 Å<sup>3</sup> which is much smaller than the symbol used to represent the data points. Inspection of the scatter in the numerically determined thermal expansion curve (see Fig. 3) suggests, however, that these standard deviations may be underestimated by a factor of about 3.

To obtain thermal expansion values in the form tabulated by Fei (1995), the data above 300 K were fitted to:

$$V(T) = V_{T_r} \exp \left[ \int_{T_r}^T \alpha(T) dT \right], \quad (1)$$

where  $V_{T_r}$  is the volume at a chosen reference temperature,  $T_r$ , and  $\alpha(T)$  is the thermal expansion coefficient, taking the form:

$$\alpha(T) = a_0 + a_1 T \quad (2)$$

This fit led to values for  $a_0$ ,  $a_1$  and  $V_{T_r}$  of  $0.375(9) \times 10^{-4} \text{ K}^{-1}$ ,  $1.4(1) \times 10^{-8} \text{ K}^{-2}$  and  $90.33(1) \text{ Å}^3$ , respectively, for a chosen  $T_r$  of 300 K.

Alternatively, if it is assumed that  $\alpha$  is independent of temperature, i.e. putting

$$\alpha(T) = \alpha_0, \quad (3)$$

we obtain  $\alpha_0 = 48.5(5) \times 10^{-6} \text{ K}^{-1}$  and  $V_{T_r} = 90.22(1) \text{ Å}^3$ , for  $T_r = 300 \text{ K}$ .

More physically meaningful interpretations of the data may be obtained using Grüneisen approximations for the zero pressure equation of state (see Wallace 1998) in which the effects of thermal expansion are considered to be equivalent to elastic strain. These take the form, to first order:

$$V(T) = \frac{\gamma' U}{K_0} + V_0, \quad (4)$$

and to second order:

$$V(T) = \frac{V_0 U}{Q - bU} + V_0, \quad (5)$$

where  $Q = V_0 K_0 / \gamma'$  and  $b = (K'_0 - 1)/2$ ;  $\gamma'$  is a Grüneisen parameter (assumed constant),  $K_0$  and  $K'_0$  are the incompressibility and its first derivative with respect to pressure, respectively, at  $T = 0$ , and  $V_0$  is the volume at  $T = 0$ . The internal energy  $U$  may be calculated using the Debye approximation (e.g. Cochran 1973) from:

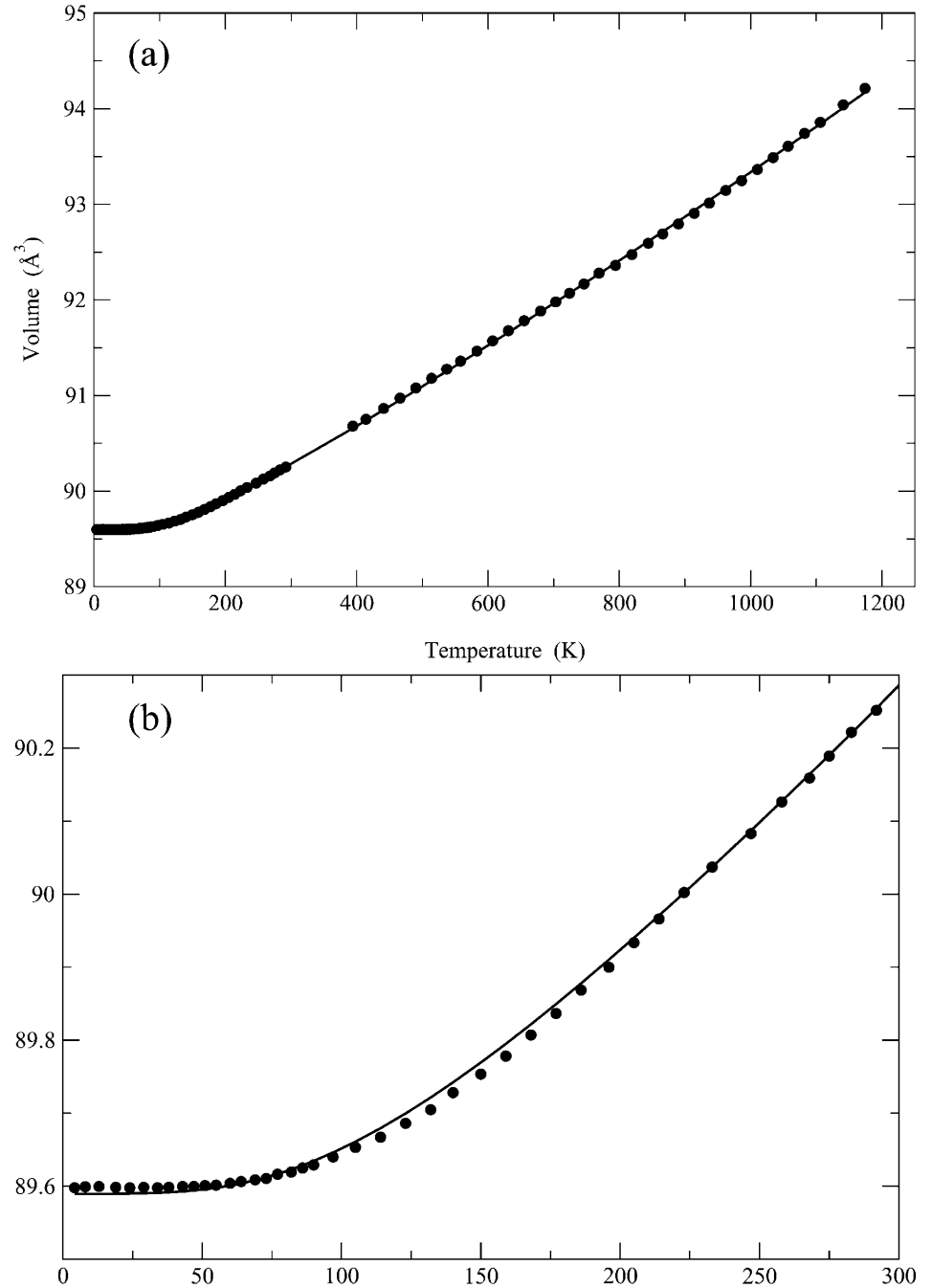
$$U(T) = 9Nk_B T \left( \frac{T}{\theta_D} \right)^3 \int_0^{\theta_D/T} \frac{x^3 dx}{e^x - 1}, \quad (6)$$

where  $N$  is the number of atoms in the unit cell,  $k_B$  is Boltzmann's constant,  $\theta_D$  is the Debye temperature.

The first-order approximation (Eq. 4) will be more valid at low temperatures where the change in  $V$  is small. It was found that Eq. (4) gave a good fit to the low-temperature (cryostat) data set with  $\theta_D = 525(6) \text{ K}$ ,  $V_0 = 89.596(8) \text{ Å}^3$  and  $\gamma'/K_0 = 1.4(1) \times 10^{-11} \text{ Pa}^{-1}$ .

In order to fit the volume data over the entire temperature range, the second-order approximation is more appropriate. The solid line in Fig. 2 shows the results obtained from using Eq. (5) with values for the four fitted constants of  $\theta_D = 445(11) \text{ K}$ ,  $V_0 = 89.590(4) \text{ Å}^3$ ,  $Q = 7.15(8) \times 10^{-18} \text{ J}$  and  $b = 1.7(2)$ . It can be seen that the fit is excellent up to a temperature of about 800 K, above which point the calculated curve is not sufficiently steep. This deviation arises from the failure of the harmonic Debye approximation at high temperatures as anharmonicity becomes increasingly important. This point is better illustrated in Fig. 3, which shows the values of the thermal expansion coefficient  $\alpha(T)$  obtained from

**Fig. 2 a** Unit-cell volume of FeSi as a function of temperature; the *solid line* shows the fit to the second-order Grüneisen approximation to the zero pressure equation of state. **b** For clarity, the low-temperature region is also shown



$$\alpha(T) = \frac{1}{V} \frac{dV}{dT} \quad (7)$$

The line in Fig. 3 shows the values of  $\alpha(T)$  calculated from differentiation of Eq. (5), whilst the points show the results obtained from simple numerical differentiation by differences of the  $V(T)$  data. The deviation of  $\alpha(T)$  from the behaviour expected using a harmonic approximation is similar to that observed in heat-capacity measurements, since the only temperature-dependent term in Eq. (5) is  $U(T)$ .

The two values of the Debye temperatures obtained from Eq. (4) and (5) [525(6) K and 445(11) K] do not

appear to be in very good agreement. However, they differ by less than the reported experimental values obtained from the coefficient of the  $T^3$  term in the temperature dependence of the specific heat-capacity data, 377 K (Paschen et al. 1997) and 596 K (Acker et al. 1999). It should also be noted that the value obtained from fitting the thermal expansion data is sensitive to the temperature range used.

A limitation of the approach described above is the assumption that the coefficients  $Q$  and  $b$  are independent of temperature; in reality this will not be the case, and the Grüneisen parameter,  $\gamma'$ , will show some temperature dependence. If we assume the value for  $K$  at

**Fig. 3** Thermal expansion coefficient of FeSi as a function of temperature. The *points* were obtained by numerical differentiation of the cell volume data; the *solid line* was obtained via Eq. (5)

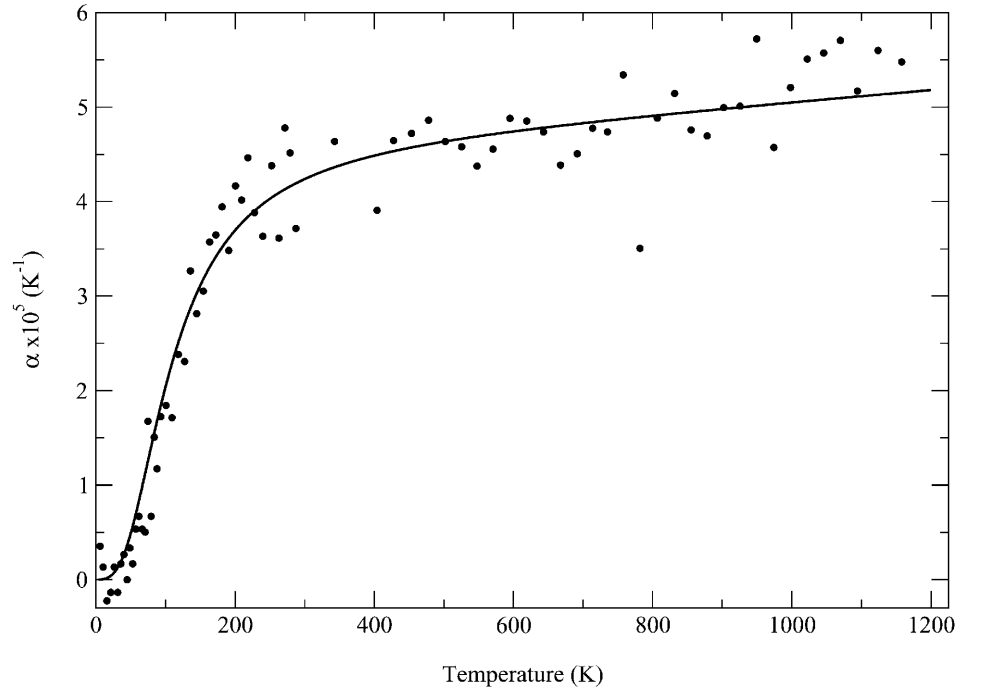
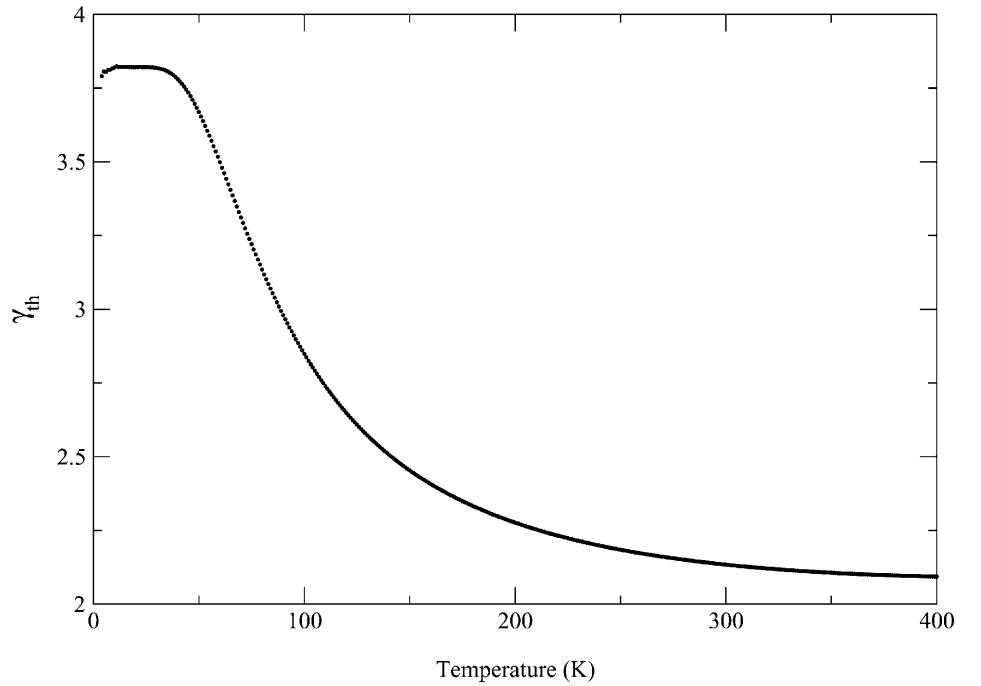


**Fig. 4** Thermodynamic Grüneisen parameter as a function of temperature determined from experimental values



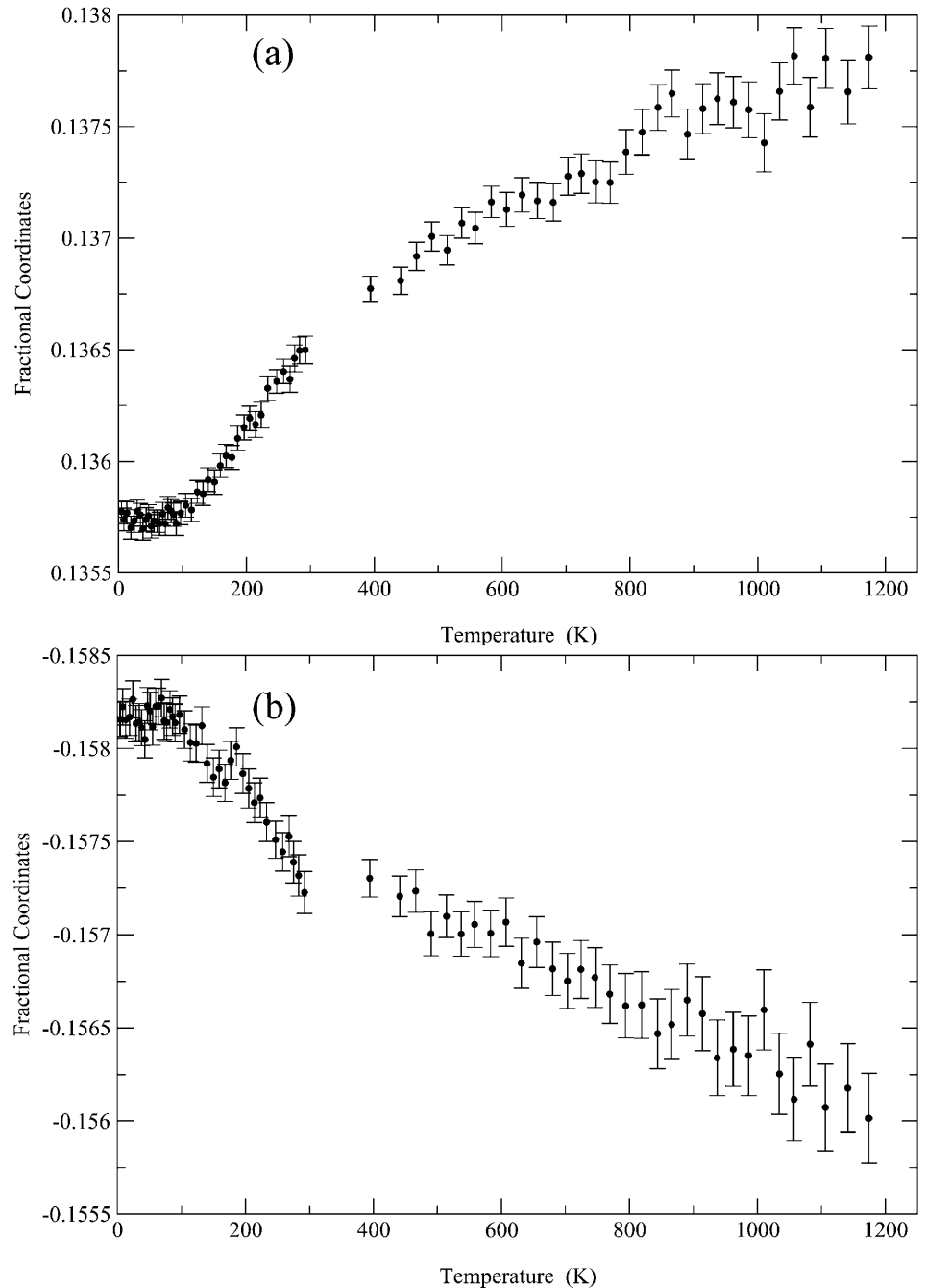
$T = 0$  (i.e.  $K_0$ ) of approximately 186 GPa determined by Sarrao et al. (1994) from resonant ultrasound spectroscopy, Eq. (4) gives  $\gamma' = 2.6(2)$  whilst Eq. (5) gives  $\gamma' = 2.33(3)$ .

There are now sufficient experimental data available to allow direct calculation of the temperature variation of the thermodynamic Grüneisen parameter, defined by:

$$\gamma_{th} = \frac{\alpha V_m K}{C} \quad (8)$$

where  $V_m$  is the molar volume,  $C$  is the molar specific heat (we assume for the purposes of the present calculations that  $C_p \sim C_v$ ),  $\alpha$  is the volume expansion coefficient and  $K$  is the incompressibility. The specific heat,  $C_p$ , has been determined by adiabatic calorimetry

**Fig. 5a, b** Temperature dependence of the fractional coordinates of **a** Fe and **b** Si atoms

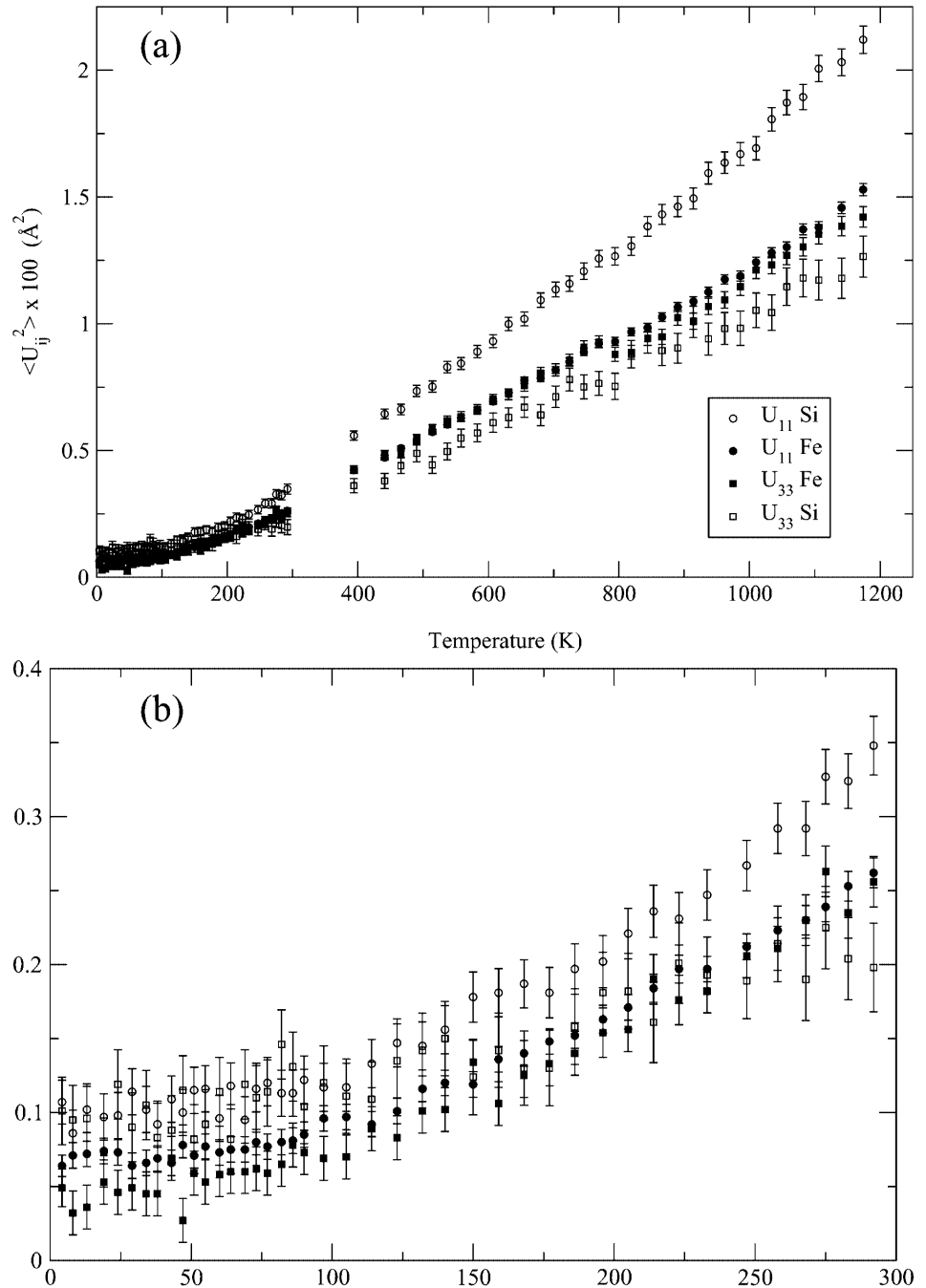


between 11 and 400 K (Acker et al. 1999) and values of  $K$  as a function of temperature may be obtained from the experimental elastic constant data of Sarrao et al. (1994). Using these measurements and the values of  $V_m$  and  $\alpha$  obtained in the present study from Eq. (5) (Figs. 2 and 3), the thermodynamic Grüneisen parameter has been calculated in the range 4 to 400 K (Fig. 4). It can be seen that  $\gamma_{th}$  is strongly temperature-dependent, but appears to be tending towards an asymptote slightly more than 2 at high temperatures. This trend is also seen in the smaller value for  $\gamma'$  (2.33) obtained above by fit-

ting the cell volume over the full temperature range as compared to that obtained from only the low-temperature data (2.6).

Equation 5 also allows determination of the pressure dependence of the incompressibility,  $K'_0$ , via the coefficient  $b$ ; the value obtained, 4.4(4), is similar to other reported values from calculations (4.2, Qteish and Shawagfeh 1998; 3.9, Vočadlo et al. 1999) and from experiments [3.5(4), Knittle and Williams 1995; 7.7(9), Wood et al. 1995 – we consider that the latter high value probably arises from the small pressure range used].

**Fig. 6 a** Principal thermal vibration parameters of Fe and Si atoms. **b** For clarity, the low-temperature region is also shown



### The effect of temperature on the crystal structure

The room temperature fractional coordinates determined in the present experiment are 0.13652(5) and  $-0.15760(9)$  for  $x_{\text{Fe}}$  and  $x_{\text{Si}}$ , respectively; these are in excellent agreement with the results from X-ray diffraction of Pauling and Soldate (1948), who obtained values of 0.137(2) and  $-0.158(4)$ . The temperature dependence of the fractional coordinates of the Fe and Si atoms is shown in Fig. 5, from which it can be seen that the structure is almost invariant with  $T$ . We do not consider the apparent break in slope in the region of

300 K shown in Fig. 5b to be of any significance; it reflects a difference in fractional coordinates from the high- and low-temperature datasets of only  $\sim 0.00025$  and probably arises from small uncorrected systematic errors introduced into the refinement by the two different sample environments. Both fractional coordinates vary in an essentially identical manner, changing by  $\sim 0.002$  ( $0.016 \text{ \AA}$ ) over the temperature range of the experiment. For both atomic species, the fractional coordinates become invariant below  $\sim 100 \text{ K}$ ; as the temperature increases from 100 K, the structure tends slightly towards the ideal sevenfold coordinated form

for which  $|x| = 0.15451$ . This latter trend is similar to that observed by experiment (Wood et al. 1996) and predicted by theory (Vočadlo et al. 1999) for the pressure dependence of the fractional coordinates of FeSi.

The temperature dependence of the principal thermal vibration parameters is shown in Fig. 6. Both the Fe and Si atoms lie on threefold axes in the crystal structure, and their probability density is, therefore, required to be an ellipsoid of revolution with one principal axis lying parallel to  $[1\ 1\ 1]$ . It can be seen that the displacements of the Fe atoms are almost isotropic at all temperatures. The probability density for the silicon, however, clearly becomes more anisotropic as the temperature increases, with the mean-squares displacements perpendicular to  $[1\ 1\ 1]$  becoming roughly twice as large as those parallel to  $[1\ 1\ 1]$ . The data shown in Fig. 6 can be fitted by a Debye-type model (e.g. Lonsdale 1962); the Debye temperatures obtained are in the range 440 to 660 K, similar in magnitude to those obtained from the lattice parameter data.

**Acknowledgements** L.V. gratefully acknowledges receipt of a Royal Society University Research Fellowship; financial support for the experiment was provided by the NERC.

## References

- Acker J, Bohmhammel K, van den Berg GJK, van Miltenburg JC, Kloc Ch (1999) Thermodynamic properties of iron silicides FeSi and  $\alpha$ -FeSi<sub>2</sub>. *J Chem Thermodynam* 31: 1523–1536
- Cochran W (1973) *The dynamics of atoms in crystals*. Arnold, London
- Fei Y (1995) Thermal expansion. In: Ahrens TJ (ed) *AGU reference shelf 2: mineral physics and crystallography – a handbook of physical constants*. AGU, Washington
- Ferrarotti A, Gail HP, Degiorgi L, Ott HR (2000) FeSi as a possible new circumstellar dust component. *Astron Astrophys* 357: L13–L16
- Hull S, Smith RI, David WIF, Hannon AC, Mayers J, Cywinski R (1992) The POLARIS powder diffractometer at ISIS. *Physica (B)* 180: 1000–1002
- Knittle E, Williams Q (1995) Static compression of  $\epsilon$ -FeSi and an evaluation of reduced silicon as a deep Earth constituent. *Geophys Res Lett* 22: 445–448
- Larson AC, Von Dreele RB (1994) GSAS (general structure analysis system). LAUR 86–748, Los Alamos Laboratory
- Lonsdale K (1962) Temperature and other modifying factors. In: MacGillavry CH, Rieck GD (eds) *International tables for X-ray crystallography*, vol. III. Kynoch Press, Birmingham
- Mattheiss LF, Hamman DR (1993) Band structure and semi-conducting properties of FeSi. *Phys Rev (B)* 47: 13114–13119
- Paschen S, Felder E, Chenikov MA, Degiorgi L, Schwer H, Ott HR, Young DP, Sarrao JL, Fisk Z (1997) Low-temperature transport, thermodynamic, and optical properties of FeSi. *Phys Rev (B)* 56: 12916–12930
- Pauling L, Soldate AM (1948) The nature of the bonds in the iron silicide FeSi and related crystals. *Acta Crystallogr* 1: 212–216
- Qteish A, Shawagfeh N (1998) A first-principles pseudopotential study of the compressibility of  $\epsilon$ -FeSi. *Sol State Commun* 108: 11–15
- Sarrao JL, Mandrus D, Migliori A, Fisk Z, Bucher E (1994) Elastic properties of FeSi. *Physica (B)* 119 and 200: 478–479
- Shirane G, Fischer JE, Endoh Y, Tajima K (1987) Temperature-induced magnetism in FeSi. *Phys Rev Lett* 59: 351–354
- Sluchanko NE, Glushkov VV, Demishev SV, Kondrin MV, Petukhov KM, Pronin AA, Samarin NA, Bruynseraede Y, Moshchalkov VV, Menovsky AA (1998) Low-temperature anomalies of the Hall coefficient in FeSi. *JETP Lett* 68: 817–822
- Tajima K, Endoh Y, Fischer JE, Shirane G (1988) Spin fluctuations in the temperature-induced paramagnet FeSi. *Phys Rev (B)* 38: 6954–6960
- Vočadlo L, Price GD, Wood IG (1999) Crystal structure, compressibility and possible phase transitions in  $\epsilon$ -FeSi studied by first-principles pseudopotential calculations. *Acta Crystallogr (B)* 55: 484–493
- Vočadlo L, Price GD, Wood IG (2000) The crystal structures and physical properties of  $\epsilon$ -FeSi-type and CsCl-type RuSi studied by first-principles pseudopotential calculations. *Acta Crystallogr (B)* 56: 369–376
- Wallace DC (1998) *Thermodynamics of crystals*. Dover, New York
- Wattanabe H, Yamamoto H, Ito K (1963) Neutron diffraction study of the intermetallic compound FeSi. *J Phys Soc Jpn* 18: 995–999
- Wood IG, Chaplin TD, David WIF, Hull S, Price GD, Street JN (1995) Compressibility of FeSi between 0 and 9 GPa, determined by high-pressure time-of-flight neutron powder diffraction. *J Phys Condens Matter* 7: L475–L479
- Wood IG, David WIF, Hull S, Price GD (1996) A high-pressure study of  $\epsilon$ -FeSi, between 0 and 8.5 GPa, by pressure time-of-flight neutron powder diffraction. *J Appl Crystallogr* 29: 215–218